Acta Pharmacologica Sinica 2017: 1554–1565
 1671-4083/17
www.nature.com/aps

Original Article

Acute liver failure enhances oral plasma exposure of zidovudine in rats by downregulation of hepatic UGT2B7 and intestinal P-gp

Fan WANG, Ming-xing MIAO, Bin-bin SUN, Zhong-jian WANG, Xian-ge TANG, Yang CHEN, Kai-jing ZHAO, Xiao-dong LIU*, Li LIU*

Center of Drug Metabolism and Pharmacokinetics, College of Pharmacy, China Pharmaceutical University, Nanjing 210009, China

HIV infection is often associated with liver failure, which alters the pharmacokinetics of many drugs. In this study we investigated whether acute liver failure (ALF) altered the pharmacokinetics of the first-line anti-HIV agent zidovudine (AZT), a P-gp/BCRP substrate, in rats. ALF was induced in rats by injecting thioacetamide (TAA, 300 mg·kg^{-1}·d^{-1}, ip) for 2 days. On the second day after the last injection of TAA, the pharmacokinetics of AZT was investigated following both oral (20 mg/kg) and intravenous (10 mg/kg) administration. ALF significantly increased the plasma concentrations of AZT after both oral and intravenous doses of AZT, but without affecting the urinary excretion of AZT. AZT metabolism was studied in rat hepatic microsomes *in vitro*, which revealed that hepatic UGT2B7 was the main enzyme responsible for the formation of AZT *O*-glucuronide (GAZT); ALF markedly impaired AZT metabolism in hepatic microsomes, which was associated with the significantly decreased hepatic UGT2B7 expression. Intestinal absorption of AZT was further studied in rats via *in situ* single-pass intestinal perfusion. Intestinal P-gp function and intestinal integrity were assessed with rhodamine 123 and FD-70, respectively. We found that ALF significantly downregulated intestinal P-gp expression, and had a smaller effect on intestinal BCRP. Further studies showed that ALF significantly increased the intestinal absorption of both rhodamine 123 and AZT without altering intestinal integrity, thus confirming an impairment of intestinal P-gp function. In conclusion, ALF significantly increases the oral plasma exposure of AZT in rats, a result partly attributed to the impaired function and expression of hepatic UGT2B7 and intestinal P-gp.

Keywords: zidovudine; acute liver failure; P-glycoprotein; UDP-glucuronosyltransferase 2B7; pharmacokinetics

Acta Pharmacologica Sinica (2017) 38: 1554–1565; doi: 10.1038/aps.2017.54; published online 3 Aug 2017

Introduction

Liver disease is caused by various pathological factors such as hepatic viruses, chemical hepatotoxins, fatty liver and autoimmune hepatitis and is a widespread pathology that in most cases leads to the down-regulation of multiple drug metabolizing enzymes[1]. Cirrhosis, for example, results in decreased total content and catalytic activity of cytochrome P450[2]. Chronic liver disease may also affect the various CYP isoforms. Using liver microsomes, George *et al* have found a decreased expression of CYP3A, 2E1, and 1A2 in severe chronic liver disease and correspondingly attenuated activities of testosterone 6β-hydroxylation (CYP3A), *N*,*N*-dimethylnitrosamine *N*-demethylation (CYP2E1) and ethoxyresorufin *O*-demethylation (CYP1A2), respectively[3]. Beyond the effects on these CYP isoforms, the activities and expression of several phase II metabolic enzymes and transporters are altered by liver disease. A recent study has shown a clear decrease in sulfotransferase 1A1, 1A3 and 1E1 activity and protein expression correlated to the extent of fatty liver disease[4]. The mRNA and protein expression of MRP2 (ABCC2) are decreased, whereas those of BCRP (ABCG2) are increased in human livers with alcoholic cirrhosis[5]. These findings suggest that the pharmacokinetic behaviors of multiple therapeutic drugs may change in liver disease. Indeed, a study of antiretroviral drugs has found that the oral plasma exposure of several HIV protease inhibitors such as indinavir, lopinavir, ritonavir, amprenavir, and atazanavir is significantly higher in patients with hepatic disease[6].

Zidovudine (AZT), belonging to the dideoxynucleoside family of nucleoside reverse transcriptase inhibitors (NRTIs), has served as a "backbone" agent for anti-HIV therapy for over 30 years[7]. Several guidelines also recommend its use as an alternative NRTI regimen in adult HIV-infected individuals who are unable to receive abacavir or tenofovir, HIV-positive pregnant women during labor, and children under 12 years of age[8-10]. Like other NRTIs, AZT competitively inhibits HIV

*To whom correspondence should be addressed.
E-mail liulee@cpu.edu.cn (Li LIU);
xdliu@cpu.edu.cn (Xiao-dong LIU)
Received 2017-01-10 Accepted 2017-04-05

reverse transcriptase or incorporates into the viral genome and terminates DNA chain expansion[11]. AZT is rapidly absorbed after oral administration[12]. It then undergoes three different types of metabolism: glucuronidation, phosphorylation, and reduction[13]. Glucuronidation is the major metabolic pathway for AZT, accounting for 60%–70% of drug clearance [13]. UDP-glucuronosyltransferase (UGT) 2B7 is probably the sole enzyme responsible for AZT glucuronidation[14]. In fact, the formation of AZT *O*-glucuronidation (GAZT) from AZT has been widely used as a specific probe reaction for UGT2B7 in glucuronidation studies[15].

A series of clinical trials with a population in liver failure have revealed the remarkable effect of hepatic dysfunction on the pharmacokinetics of AZT. Patients with hepatic dysfunction in a single-dose pharmacokinetic study of AZT showed an elevated area under the curve (AUC) and an earlier maximum plasma concentration (C_{max}) of AZT[16]. In a study of 14 HIV-negative subjects, those with cirrhosis had a marked decrease in oral clearance and an increase in the C_{max}, half-life ($t_{1/2}$) and mean residence time (MRT)[17]; HIV-infected individuals with mild liver disease, compared with healthy subjects, have been reported to have a relatively smaller decrease in the oral clearance of AZT[18]. The increased plasma exposure of AZT after oral administration in patients with hepatic dysfunction has been identified from the decreased glucuronidation of AZT in subjects with liver disease[19]. However, the mechanism underlying the altered pharmacokinetics of AZT under liver failure remains unclear. For example, accumulating data show that AZT is a substrate for ATP-binding cassette drug transporters, including P-glycoprotein (P-gp) and breast cancer resistance protein (BCRP)[20-22], which are widely distributed on the apical membranes of cells in the intestinal epithelia, liver, and blood-brain barrier. These membranes act as defenders against numerous exogenous and endogenous substances. Our previous study has also indicated that acute liver failure (ALF) impairs the function and expression of P-gp and BCRP at the blood-brain barrier in rats, thus resulting in increased brain distributions of rhodamine 123 and prazosin[23, 24]. However, information on intestinal P-gp and BCRP functions and expression under liver failure status is lacking. These changes may also contribute to the altered pharmacokinetics of AZT during liver failure. The aim of this study was to investigate the effects of ALF on the pharmacokinetics of AZT and to explore the possible underlying mechanisms.

Materials and methods

Chemicals

Thioacetamide (TAA) was purchased from J&K Scientific Ltd (Beijing, China). Zidovudine (AZT), and AZT *O*-glucuronide (GAZT) were purchased from Santa Cruz Biotechnology, Inc (Santa Cruz, CA, USA). Fluorescein isothiocyanate-conjugated (FITC) dextran 70 kDa (FD-70), rhodamine 123 and prazosin were purchased from Sigma Aldrich (St Louis, MO, USA). Kits for the activity assays of alanine amino transferase (ALT), aspartate amino transferase (AST), alkaline phosphatase (ALP), superoxide dismutase (SOD), catalase (CAT) and glutathione peroxidase (GSH-Px) and for the content determinations of total bilirubin, conjugated bilirubin, ammonia, tumor necrosis factor alpha (TNF-α), malondialdehyde (MDA), creatinine and urea nitrogen were purchased from Jiancheng Bioengineering Institute (Nanjing, China). A bicinchoninic acid (BCA) kit for protein quantitation was purchased from the Beyotime Institute of Biotechnology (Haimen, China). Mouse monoclonal antibodies specific to P-gp (clone C219) were purchased from Calbiochem-Novabiochem (Seattle, WA, USA), and antibodies to BCRP and β-actin were purchased from Abcam (Cambridge, UK). Mouse monoclonal antibodies to UGT2B7 were purchased from Novus Biologicals (Littleton, CO, USA). Water was purified using a Milli-Q system (Millipore, Bedford, USA). All other chemicals used were commercially available and of analytical grade.

Animals

Male Sprague-Dawley (SD) rats weighing 180–220 g were purchased from Sino-British Sipper & BK Lab Animal Co., Ltd (Shanghai, China). The rats were housed in a controlled environment (temperature of 23±1 °C and relative humidity of 50%±10% with a 12-h light/darkness cycle) and were allowed free access to water and food. The animals were acclimated to the facilities for 5 days and fasted and given free access to water for 12 h prior to the experiment. All experiments were carried out according to the Institutional Guidelines for the Care and Use of Laboratory Animals and were approved by the Animal Ethics Committee of China Pharmaceutical University.

Induction of ALF in rats

ALF in rats was induced with thioacetamide (TAA) according to a previously established method[24, 25]. Briefly, male SD rats, weighing 260–280 g, were intraperitoneally administered injections of TAA (300 mg/kg) for two successive days with a 24-h interval. Control rats received only physiological saline (vehicle). To minimize hypoglycemia and electrolyte imbalances, drinking water containing 5% dextrose, 0.45% NaCl and 0.149% KCl was provided to all rats as supportive therapy[26]. All experiments were performed 24 h after the last injection of TAA or vehicle.

Pharmacokinetics of AZT in ALF and control rats after oral and intravenous administration

On the second day after the last injection of TAA, ALF and age-matched control rats were orally administered 20 mg/kg AZT. The dose of zidovudine for oral administration was based on a previous study[27]. Blood samples (approximately 0.2 mL) were collected under light ether anesthesia via the postorbital venous plexus veins into heparinized tubes at 5, 10, 20, 30, 45, 60, 120, 240, 360, 480 and 600 min after the oral dose of AZT. After 3 or 4 samplings, the equivalent amount of normal saline was administered to the rats via the tail vein to compensate for the blood loss. After blood was centrifuged at 5000 r/min for 5 min, the plasma samples were obtained and frozen at -20 °C until analysis.

For intravenous administration, AZT (10 mg/kg) was

administered to ALF and control rats via the caudal vein. The dose of zidovudine for intravenous administration (10 mg/kg) was based on several published studies[28, 29]. Blood samples (approximately 0.2 mL) were collected at 5, 10, 15, 30, 45, 60, 120, 180, 300 and 420 min after administration of the intravenous dose under light ether anesthesia. The collection and the treatment of blood samples were performed by using the same method as described for oral administration.

Effect of ALF on the urinary excretion of AZT

For urinary excretion, ALF and age-matched control rats were housed individually in metabolic cages before the study. After a 24-h adaptation period, rats received an intravenous administration of AZT (10 mg/kg). Urine samples were collected before dosing and at intervals of 0–3 h, 3–6 h, 6–9 h, 9–12 h, and 12–24 h after dosing. Aliquots of urine samples were stored at -80 °C until analysis.

Determination of biochemical and physiological parameters

The experimental rats, fasted overnight, were sacrificed under light ether anesthesia. Blood and tissues (liver and intestine) were immediately collected for the determination of biochemical parameters, histological analysis and Western blotting. Parts of the liver were used for preparing hepatic microsomes. Body and liver weights were measured to verify the induction of ALF. The levels of ALT, AST, AKP, total bilirubin, conjugated bilirubin, TNF-α, ammonia, creatinine and urea nitrogen in serum, as well as the levels of GSH-Px, CAT, SOD and MDA in liver, were measured using commercial reagent kits following the manufacturer's instructions.

Histological analysis of liver and intestine

The same parts of the liver and intestine were excised from ALF and control rats, sliced into -0.3 to -0.5 cm sections and immersed in a 10% formalin solution for fixation. After dehydration with alcohol, the tissue specimens were embedded in paraffin. After the solidification, specimens were cut into 4-μm slices, stained with hematoxylin-eosin (H&E) and observed by light microscopy.

The preparation of hepatic microsomes and the metabolism of AZT in hepatic microsomes

Hepatic microsomes were freshly prepared from the ALF and control rats mentioned above according to previously described methods[30]. The rats were sacrificed under light ether anesthesia, and their livers were quickly harvested. The microsomal pellets were resuspended in 0.1 mol/L phosphate-buffered saline (pH 7.4) containing 30% glycerol and were stored at -80 °C. The protein concentrations were measured with a BCA protein assay kit.

AZT metabolism in the hepatic microsomes of rats was assessed by measuring the formation of GAZT. Briefly, hepatic microsomes (1 mg/mL) were incubated for 30 min at 37 °C with AZT (0.5, 1 and 2 mmol/L) and an UDPGA-generating system (5 mmol/L UDPGA, 5 mmol/L saccharolactone, 80 μg/mL Triton-X 100, and 10 mmol/L $MgCl_2$) in a final volume of 100 μL. The AZT concentration (2 mmol/L) was below its K_m value (9.1 mmol/L)[31]. The reaction was terminated by addition of 100 μL of ice-cold acetonitrile containing 0.2% formic acid. All incubations were performed in triplicate. The amount of GAZT formed in the reaction mixture was determined.

In human hepatic microsomes, the formation of GAZT was considered to be mediated by UGT2B7[32]. To investigate whether UGT2B7 was also the main enzyme responsible for AZT metabolism in rats, the effect of an anti-UGT2B7 polyclonal antibody on the formation of GAZT was also documented. Briefly, the rabbit anti-rat UGT2B7 polyclonal antibody was preincubated with rat hepatic microsomes for 20 min at room temperature, and AZT (2 mmol/L) was then added. The mixture was prepared, and the process was performed according to the methods described above.

Western blot analysis

The protein levels of liver UGT2B7 and intestinal P-gp and BCRP were assessed by Western blotting[33, 34]. Briefly, the livers and intestines were homogenized in RIPA lysis buffer (containing 1 mmol/L phenylmethylsulfonyl fluoride, PMSF) and diluted with loading buffer as previously described. Seventy micrograms of protein was loaded into each lane of the sodium dodecyl sulfate-polyacrylamide gel, separated by electrophoresis and transferred to polyvinylidene fluoride membranes (Millipore Corporation, Billerica, MA, USA). Blots were blocked in 5% skimmed milk-TBST (Tris buffer saline-Tween 20) for 2 h at room temperature and then washed. After incubation with primary antibodies overnight at 4°C, the membranes were incubated with horseradish peroxidase-conjugated secondary antibodies for 2 h. The immunoreactivity was detected using a chemiluminescent substrate (Thermo Fisher Scientific Inc, Rockford, IL, USA) and a gel imaging system (Tanon 5200 multi system, Shanghai, China). The levels of the target proteins were normalized to levels of β-actin as a reference. The primary antibodies used were to BCRP (1:200 dilution), P-gp (1:50 dilution), UGT2B7 (1:500 dilution) and β-actin (1:5000 dilution).

Effects of ALF on the absorption of AZT and rhodamine 123

The effects of ALF on AZT absorption were evaluated by *in situ* single-pass perfusion as previously described[35]. Briefly, rats were fasted overnight and anesthetized with 60 mg/kg pentobarbital (ip). After the isolation of 20 cm of jejunum, two cannulas were inserted into either end (input and output). The isolated jejunum was flushed with blank Krebs-Henseleit buffer (37 °C) at a fast rate for 10 min, then with Krebs-Henseleit buffer containing 10 μmol/L AZT or 0.5 μmol/L rhodamine 123 at a 0.2 mL/min flow rate until equilibrium was reached. The total perfusion period was 120 min, and efflux samples were collected every 15 min from the output cannula. Rats were sacrificed at the end of the perfusion, and the perfused segments were removed for measurements of the absorption areas. The apparent effective permeability (P_{eff}, cm/min) was calculated with the following equation: $P_{eff}=-Q\cdot$

ln (C_{out}/C_{in})/A, where Q is the entering intestinal perfusion flow rate, C_{in} and C_{out} are the concentration of AZT or rhodamine 123 in the inlet and outlet perfusates and A represents the absorption areas of the isolated jejunum. A deviation in C_{out} caused by water absorption was corrected by using a gravimetric method[36].

Intestinal integrity in ALF and control rats

In vivo intestinal integrity was measured using a previously described method[37]. Rats received oral gavages of fluorescein isothiocyanate (FITC)-labeled 70-kDa dextran (FD-70) at 50 mg/kg body weight in phosphate-buffered saline (PBS, pH 7.4). After 1 and 4 h, 100 μL of blood were collected from the postorbital venous plexus veins. Plasma was obtained by the addition of 10 μg/mL heparin and centrifugation at 5000×*g* for 5 min at 4 °C. Plasma (50 μL) was mixed with an equal volume of PBS (pH 7.4) and added to a 96-well microplate. The concentration of fluorescein was determined by spectrophotometry (Varioskan Flash, Thermo Scientific, USA) with an excitation wavelength of 485 nm and an emission wavelength of 525 nm, using a calibration curve.

Analytical procedures

The concentrations of AZT and GAZT in plasma or urine were determined using liquid chromatography tandem mass spectrometry (LC-MS) according to a previously described method[38]. The linear ranges of AZT and GAZT in plasma were 0.05–10 μg/mL and 0.025–2 μg/mL, and the lowest limits of quantification of AZT and GAZT were 50 ng/mL and 25 ng/mL, respectively. The linear ranges of AZT and GAZT in urine were 0.05–10 μg/mL and 0.025–5 μg/mL, and the lowest limits of quantification of AZT and GAZT were 50 ng/mL and 25 ng/mL, respectively. The recoveries were higher than 80%, and the relative standard deviations of the intra- and inter-assays were lower than 10%.

Measurement of GAZT in the incubation mixtures was performed according to a previously reported method[39], with slight modification. Briefly, 10 μL of terazosin (internal standard, 25 μg/mL) was added to 200 μL of the microsomal incubation mixture, and the mixture was centrifuged at 20000 ×*g* for 10 min. The supernatant was injected into an LC-MS system. The mobile phase consisted of acetonitrile and water (17:83, *v/v*). Detection was performed on a triple quadrupole tandem mass spectrometer equipped with an electrospray ionization source operated in selected reaction monitoring mode (*m/z* 442.00→125.00 for GAZT and *m/z* 388.15→290.20 for the IS terazosin). The detection limit for GAZT was 0.02 μmol/L, and the recoveries were greater than 75%. The intra-day and inter-day coefficients of variation for the assay were less than 10%.

The concentrations of AZT and rhodamine 123 in the intestinal eluate samples were determined using ultraviolet and fluorescence HPLC detectors, respectively, according to previously described methods[40, 41]. The lowest limits of quantification of AZT and rhodamine 123 in the intestinal eluate samples were 0.5 and 0.02 μmol/L, respectively. The linear ranges of AZT and rhodamine 123 in intestinal eluate samples were 0.5–40 μmol/L and 0.02–1 μmol/L, respectively. The recoveries of AZT and rhodamine were higher than 85%, and the relative standard deviations of the intra-day and inter-day levels in the samples were lower than 10%.

Statistical analysis

The pharmacokinetic parameters were estimated using a non-compartmental analysis (Pheonix Winnonlin 6.4, Pharsight, St Louis, MO, USA). If the data fit a normal distribution, a standard analysis of variance was used. The significance of differences between two groups was determined with Student's *t*-test. If the data were not normally distributed, a Mann-Whitney U test was used for a comparison between two groups. All results are expressed as the mean±standard deviation (SD).

Results

Alterations of biochemical parameters and histopathological characteristics in ALF rats

ALF induced by thioacetamide was confirmed on the basis of the physiological and biochemical parameters listed in Table 1. The increased levels of ALT and AST were used as markers to ascertain liver failure. In the sera of the TAA-treated rats, compared with the control rats, an 8-fold increase in AST and a 9-fold increase in ALT were observed. Along with the increased ALT and AST levels, the serum AKP, total bilirubin, conjugated bilirubin and TNF-α levels in ALF rats were also significantly elevated compared with the levels in the control rats. However, the serum ammonia, creatinine and urea nitrogen levels were not affected by TAA-induced ALF.

The GSH-Px, MDA, SOD and CAT levels in the livers were also measured (Table 1) as indicators of oxidative stress. No differences in the liver SOD levels were found between the groups. However, in the ALF rats, compared with the control rats, significantly decreased levels of GSH-Px and CAT but increased levels of MDA were observed in the liver, thus indicating that oxidative stress was induced in the livers of ALF rats.

The histopathological characteristics of the liver and intestine were assessed by light microscopic examination (Figure 1). The livers from ALF rats showed severe vacuolation and inflammatory infiltration. The results of the biochemical parameters and histopathological studies suggested that the rat liver function was impaired by piecemeal necrosis after TAA administration. However, histopathological evaluation of the jejunum revealed no overt differences between ALF and control rats.

Effects of ALF on the pharmacokinetics of AZT in rats

The plasma concentration of AZT after oral administration of 20 mg/kg AZT to rats is shown in Figure 2A, and the estimated pharmacokinetic parameters of AZT are listed in Table 2. Higher concentrations of AZT were found in ALF rats. The mean $AUC_{(0-10\ h)}$ in ALF rats was significantly higher than that in the control rats (16.14±2.52 μg · h/mL in ALF rats *vs* 10.74±1.28 μg · h/mL in control rats). This result indicated that ALF may increase the plasma exposure of AZT after oral administration.

Table 1. Physiological and biochemical parameters of the acute liver failure (ALF) rats and age-matched control (CON) rats. Data are expressed as mean±SD. n=6. $^{*}P$<0.05, $^{**}P$<0.01 *vs* CON rats.

Parameters	CON	ALF
Physiological parameters		
Body weight (BW) (g)	252.63±12.70	232.70±11.94**
Liver weight (% BW)	2.99±0.42	4.47±0.26**
Serum		
ALT (IU/L)	27.39±4.15	250.08±47.44**
AST (IU/L)	46.03±15.01	377.03±85.29**
AKP (IU/L)	165.83±45.60	316.03±82.37**
Total bilirubin (μmol/L)	3.39±1.25	6.13±2.48**
Conjugated bilirubin (μmol/L)	1.59±1.48	4.09±2.87**
TNF-α (pg/mL)	7.69±3.10	130.88±40.90**
Ammonia (μmol/L)	76.85±18.78	88.53±21.33
Creatinine (μmol/L)	44.83±15.15	47.17±17.63
Urea nitrogen (mmol/L)	4.89±1.18	5.38±1.05
Liver		
GSH-Px (units/mg protein)	183.97±41.75	122.28±24.20*
CAT (units/mg protein)	25.75±7.21	16.62±4.43*
SOD (units/mg protein)	42.66±7.46	41.02±6.91
MDA (nmol/mg protein)	2.87±0.72	4.21±0.80*

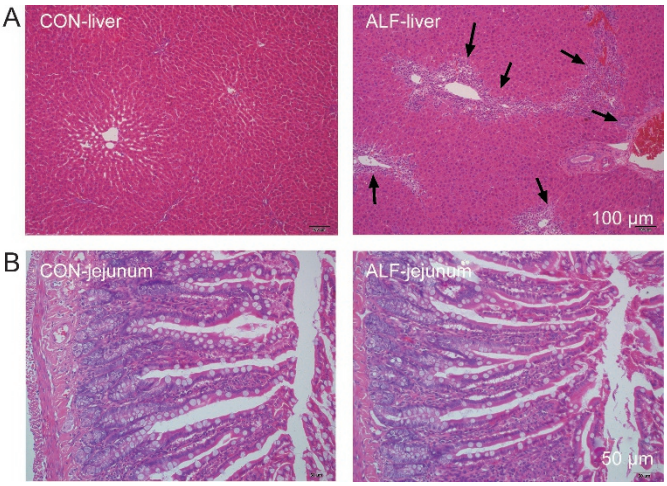

Figure 1. Histological analyses of liver (A) and jejunum (B) from acute liver failure (ALF) rats and age-matched control (CON) rats. All sections were stained with hematoxylin-eosin (magnification, 200× for jejunum and 100× for liver). Scale bar represented 100 μm for liver and 50 μm for jejunum, respectively. Arrows indicate vacuolation and inflammatory cell infiltration.

To investigate whether the higher oral exposure of AZT in ALF rats resulted from decreased system clearance, the pharmacokinetics of AZT and its main metabolite, GAZT, were also studied in ALF and control rats after intravenous administration of AZT (10 mg/kg) (Figure 2B and 2C). Similarly to the results after oral administration, higher plasma exposure of AZT was found in ALF rats. The $AUC_{0-\infty}$ of AZT in ALF rats was 1.5-fold of that in the control rats, and the half-life ($t_{1/2}$) of AZT in ALF rats was much longer than that in the control rats. However, the plasma concentrations and AUC of GAZT were markedly decreased in ALF rats compared with the control rats (0.43±0.06 μg·h/mL in ALF rats *vs* 0.69±0.14 μg·h/mL in the control rats). These results indicated that AZT was more slowly metabolized and eliminated in ALF rats than in the control rats and was accompanied by lower system clearance.

Table 2. Pharmacokinetic parameters of zidovudine (AZT) after oral administration of 20 mg/kg AZT or intravenous administration of 10 mg/kg AZT to acute liver failure (ALF) rats and age-matched control (CON) rats. Data are expressed as mean±SD. n=6. $^{*}P$<0.05, $^{**}P$<0.01 *vs* CON rats.

Group	CON	ALF
Oral administration		
k (1/h)	0.65±0.08	0.37±0.04**
$t_{1/2}$ (h)	1.07±0.15	1.91±0.22**
T_{max} (h)	0.71±0.10	0.54±0.10*
C_{max} (μg/mL)	5.72±0.70	7.76±0.88**
AUC_{0-t} (μg·h·mL^{-1})	10.74±1.28	16.14±2.52**
$AUC_{0-\infty}$ (μg·h·mL^{-1})	10.82±1.29	16.53±2.52**
V_z/F (L/kg)	2.89±0.44	3.43±0.89
CL/F (L·h^{-1})	1.87±0.23	1.23±0.19**
MRT (h)	1.83±0.19	2.55±0.11**
Intravenous administration		
k (1/h)	1.57±0.13	0.88±0.13**
$t_{1/2}$ (h)	0.44±0.04	0.80±0.13**
C_0 (μg/mL)	14.15±2.52	17.74±3.83**
AUC_{0-t} (μg·h·mL^{-1})	8.09±1.42	12.39±1.28**
$AUC_{0-\infty}$ (μg·h·mL^{-1})	8.17±1.43	12.57±1.34**
V_z (L/kg)	0.76±0.16	0.75±0.06
CL (L·h^{-1})	1.25±0.20	0.80±0.08**
MRT (h)	0.61±0.07	0.94±0.08**

Effects of ALF on the urinary excretion of AZT and GAZT in rats

Previous studies have demonstrated that urinary excretion of the parent drug (approximately 70% of the oral or intravenous dose) is the primary excretive pathway of AZT in rats[42, 43]. Thus, urinary excretion of AZT and GAZT after intravenous administration was determined, to investigate whether the increased exposure of AZT in ALF rats resulted from decreased urinary excretion of AZT. The results showed that trace amounts of GAZT were excreted in the urine (Figure 2E), whereas a large amount of AZT was detected, which accounted for approximately 55%–60% of the intravenous dose (Figure 2D). The contribution of the urinary excretion of GAZT to the overall AZT elimination was limited (only 2% of the intravenous dose), and ALF did not affect the urinary excretion of either AZT or GAZT.

Metabolism of AZT in the hepatic microsomes of ALF rats

AZT is a classic UGT substrate and is metabolized to an inactive compound, GAZT, by hepatic UGT enzymes, primarily UGT2B7 in humans. To verify whether UGT2B7 contributed to AZT metabolism in rats, the formation rates of GAZT in

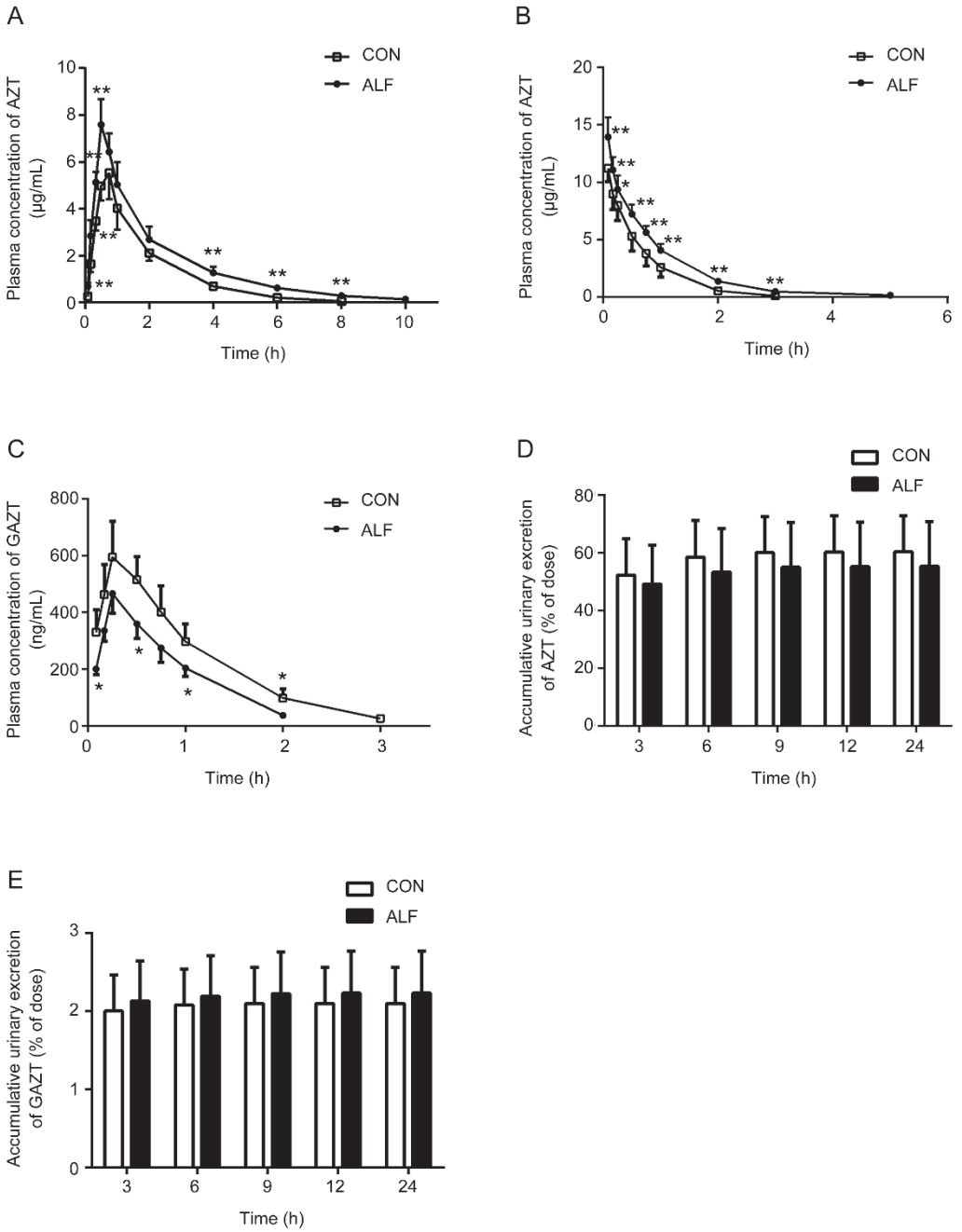

Figure 2. Plasma concentration-time profiles of zidovudine (AZT) and AZT *O*-glucuronide (GAZT) following oral administration of 20 mg/kg of AZT (A) or intravenous administration of 10 mg/kg of AZT (B, C) to acute liver failure (ALF) rats (●) and age-matched control (CON) rats (□). The accumulative excretion of AZT (D) and GAZT (E) via urine following intravenous AZT (10 mg/kg) in ALF rats (shaded bar) and CON rats (white bar). Data are expressed as mean±SD. n=6. $^{*}P$<0.05, $^{**}P$<0.01 *vs* CON rats.

rat hepatic microsomes were investigated in the presence or absence of an anti-UGT2B7 antibody (Figure 3A). The results showed that an antibody against UGT2B7 inhibited AZT metabolism. The formation rate of GAZT in the presence of the antibody against UGT2B7 (20 μL/mg microsomal protein) was 19.3±4.2 pmol·min^{-1}·mg^{-1} protein, a value significantly lower than that in the absence of the anti-UGT2B7 antibody (40.1±4.8 pmol·min^{-1}·mg^{-1} protein). The results indicated that in rats, similarly to humans, UGT2B7 was responsible for the formation of GAZT.

To investigate whether the increased plasma concentration of AZT in ALF rats resulted from impaired UGT2B7 activity, the UGT2B7 activity in the hepatic microsomes of ALF rats was determined by measuring the formation of GAZT from AZT, a specific *in vitro* probe. As shown in Figure 3B, compared with those in the control rats, the hepatic microsomes

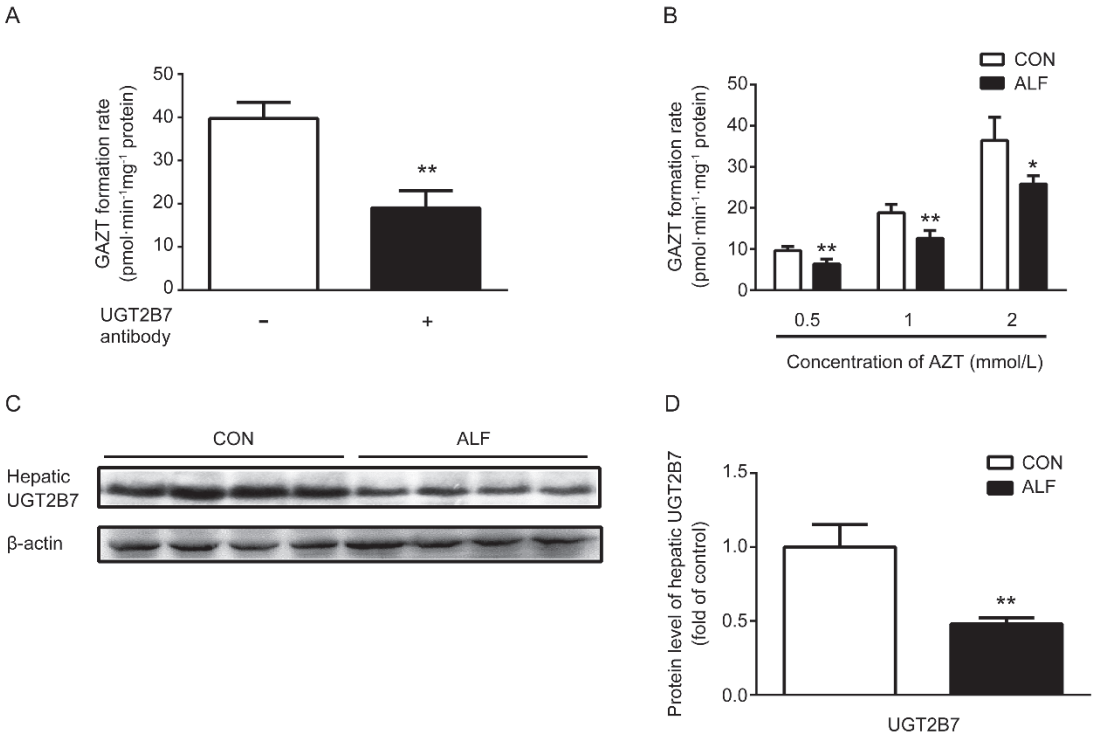

Figure 3. Effect of acute liver failure (ALF) on zidovudine (AZT) metabolism and UGT2B7 expression in hepatic microsomes. (A) The effects of an antibody to UGT2B7 on the formation of GAZT in the hepatic microsomes of CON rats. (B) The formation of zidovudine *O*-glucuronide (GAZT) in the hepatic microsomes of ALF rats (shaded bar) and age-matched control (CON) rats (white bar). The relative protein expressions (C) and the corresponding quantitative results (D) of hepatic UGT2B7 in ALF rats (shaded bar) and CON rats (white bar). Data are expressed as mean±SD. n=4. $^{*}P$<0.05, $^{**}P$<0.01 *vs* CON rats.

of ALF rats showed significant decreases in the formation of GAZT, thus suggesting impairment of the hepatic UGT2B7 activity. Western blotting also demonstrated that the protein expression of hepatic UGT2B7 in ALF rats was significantly decreased to only 35% of that in the control rats (Figure 3C and 3D). The decreased expression of UGT2B7 in the hepatic microsomes of ALF rats was consistent with the attenuation of GAZT production, thus indicating that the increased plasma exposure of AZT might partly result from the decreased activity and expression of hepatic UGT2B7 in ALF rats.

Effects of ALF on the expression of intestinal P-gp and BCRP

AZT is a substrate of both P-gp and BCRP. To investigate the contributions of intestinal BCRP and P-gp to the enhanced oral absorption of AZT in ALF rats, the levels of the intestinal P-gp and BCRP proteins in ALF and age-matched control rats were compared by western blot analysis. The intestinal P-gp expression in ALF rats significantly decreased, to 35% of that in the control rats. In contrast, the BCRP expression in ALF rats showed a slight increase but no significant difference compared with that in the control rats (Figure 4).

Effects of ALF on the intestinal absorption of AZT and rhodamine 123

We further investigated whether the higher exposure of AZT

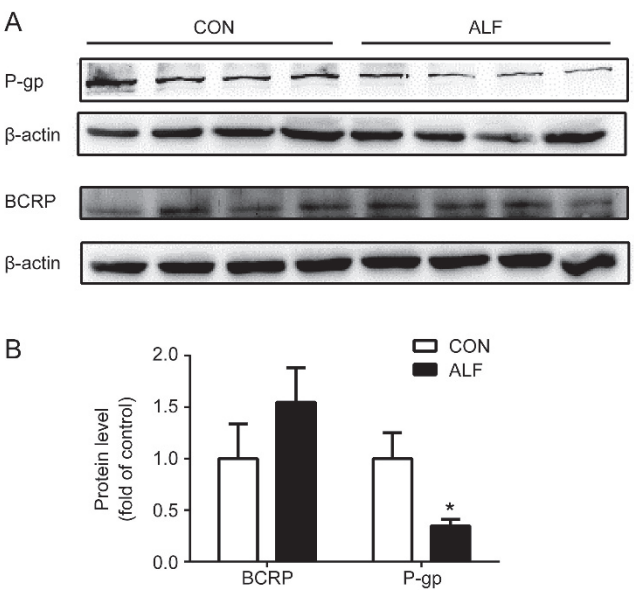

Figure 4. The relative protein expression (A) of intestinal P-gp and BCRP in acute liver failure (ALF) rats (shaded bar) and age-matched control (CON) rats (white bar). Quantification of Western blotting of intestinal P-gp and BCRP (B) in ALF rats (shaded bar) and CON rats (white bar) are shown, respectively. Data are expressed as mean±SD. n=4. $^{*}P$<0.05 *vs* CON rats.

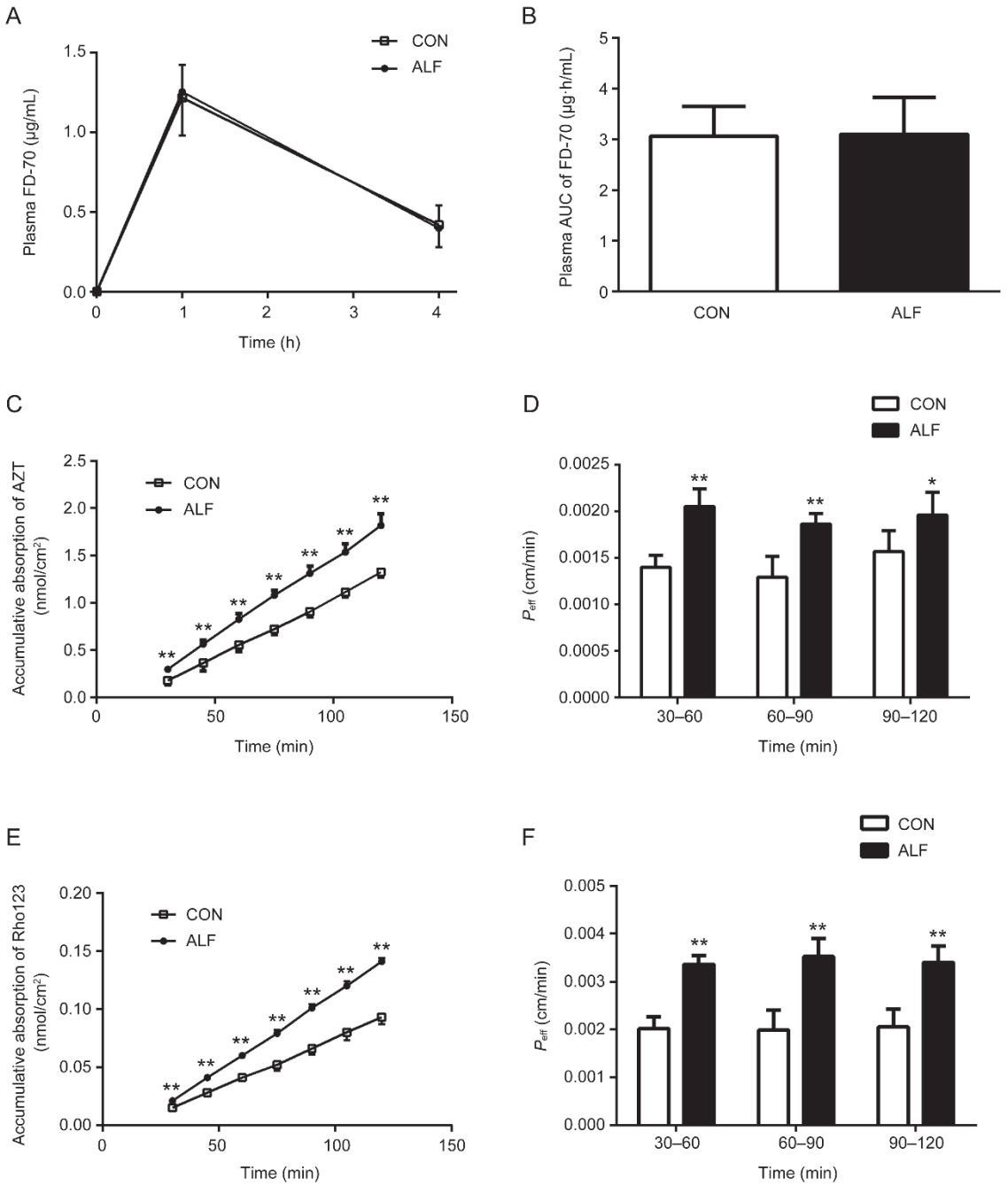

Figure 5. The effects of acute liver failure (ALF) on intestinal permeability and the absorption of zidovudine (AZT) and rhodamine 123 in the jejunum of rats. Plasma fluorescein isothiocyanate-conjugated (FITC) dextran 70 kDa (FD-70) levels (A) and the corresponding AUC of FD-70 (B) were measured 1 and 4 h after oral administration of FD-70 (50 mg/kg) in ALF rats (●, shaded bar) and age-matched control (CON) rats (□, white bar). The accumulative absorption of AZT (C) and rhodamine 123 (E), the corresponding P_{eff} of AZT (D) and rhodamine 123 (F) were measured using an *in situ* single-pass intestinal perfusion in ALF rats (●, shaded bar) and CON rats (□, white bar), respectively. Data are expressed as mean±SD. n=6. $^{*}P$<0.05, $^{**}P$<0.01 *vs* CON rats.

in ALF rats after oral administration resulted from an increase in AZT absorption across the intestine. Comparative studies of the intestinal absorption of AZT in ALF and control rats were performed by using *in situ* single-pass intestinal perfusion (Figure 5C and 5D). The results showed that the intestinal absorption of AZT in ALF rats was significantly higher than that in the control rats. At 120 min, the accumulative absorption of AZT in ALF rats reached 1.37-fold of that in the control rats (1.82±0.126 nmol/cm^2 in ALF rats *vs* 1.32±0.052 nmol/cm^2 in control rats). The P_{eff} values of AZT in ALF rats were increased by approximately 47%, 44% and 25% at 60 min, 90 min and 120 min, respectively, relative to the control rats.

This result indicated that the higher exposure of AZT after oral administration resulted from increased oral absorption of AZT across the intestine.

To examine whether the increased oral absorption of AZT was caused by impairment of the intestinal barrier, the integrity of the intestinal barrier was assessed by using FD-70, a fluorescein-labelled dextran. The results showed that plasma concentrations of FD-70 in ALF rats were comparable to those of control rats (Figure 5A and 5B), a result consistent with the histopathological results (Figure 1B), thus indicating that ALF did not affect the integrity of the intestinal barrier and that the increased oral absorption of AZT across the intestine did not result from the damaged intestinal integrity.

It is generally accepted that AZT is a P-gp and BCRP substrate. Data from the Western blots showed that ALF also downregulated the expression of intestinal P-gp. Rhodamine 123, a classical P-gp substrate, was used to evaluate the function of P-gp. As shown in Figure 5E and 5F, the accumulative absorption and P_{eff} values of rhodamine 123 in the ALF rats were significantly increased compared with those in the control rats. This result was consistent with the decreases in expression of the intestinal P-gp protein and indicated that the increased absorption of rhodamine 123 and AZT in ALF rats was attributable to the impaired function and expression of intestinal P-gp.

Discussion

The TAA-induced ALF rat model was used in this study. This model has been widely used and is well established for liver function assessments, because it resembles several pathophysiological and clinical features of ALF in humans[44]. As expected, TAA treatment was accompanied by liver failure, as indicated by increased serum levels of liver enzymes (AST and ALT), AKP, TNF-α and total bilirubin, though serum ammonia levels were not changed by ALF. In addition, oxidative stress was observed in the livers of hepatotoxic rats, as evidenced by increased MDA levels and decreased GSH-Px and CAT levels in liver tissue homogenates. On the basis of the unchanged creatinine and urea nitrogen levels in the serum, renal function might not have been influenced by ALF.

This study showed that the oral AUC of AZT in ALF rats was significantly higher than that in control rats, a result consistent with the AZT pharmacokinetics reported in patients with liver disease[45]. To investigate whether the higher oral AUC in ALF rats was a consequence of decreased systemic clearance, the AUC of AZT and its metabolite GAZT were estimated after intravenous administration of AZT. In accordance with our hypothesis, an increased AUC of AZT and a decreased AUC of GAZT were found in ALF rats after intravenous administration, thus indicating that the ALF condition decreased the systemic clearance of AZT. However, the plasma concentrations and systemic exposure of GAZT were significantly lower than those of AZT in both ALF and control rats, results markedly different from the data in humans. The pharmacokinetics of AZT and GAZT have been studied in healthy volunteers and patients with liver cirrhosis or HIV-infections[13, 17]. After oral administration of AZT, the mean plasma levels of GAZT were between 2 and 5 times greater than those of the parent drug. These results indicated that the ability for the catalysis of AZT to GAZT in humans may be distinct from that in rats.

To investigate whether the increased exposure of AZT in ALF rats resulted from decreased urinary excretion of AZT, the urinary excretion of AZT and GAZT after intravenous administration of AZT was measured. The results also differed from those in humans. The percentage of the dose recovered in human urine as AZT and GAZT is 10%–20% and 60%–70%, respectively, after oral or intravenous administration[46, 47]. However, in our study, only trace amounts of GAZT (approximately 2% of the intravenous dose) were excreted in the urine, whereas a large amount of the parent drug, AZT (approximately 60% of the intravenous dose), was detected in the urine samples of both ALF and control rats. A previous study has also found that urinary excretion of AZT, as unchanged drug, in rats accounted for 70% of the intravenous dose but that only 1% of the dose was recovered in the urine as GAZT[42], in agreement with our results. The urinary excretion of AZT and GAZT was not influenced by ALF in rats. These results were in accord with the findings that the plasma exposure of GAZT was significantly lower than that of AZT. The excretive experiment also revealed interspecies differences in the metabolism and excretion of AZT between humans and rats.

AZT undergoes glucuronidation to AZT *O*-glucuronidation (GAZT) as the major metabolic pathway after absorption both in humans and rats and is catalyzed mainly by UGT2B7 in humans[32]. However, the UGT isoforms responsible for AZT glucuronidation in rats have not been fully characterized. A previous study has also authenticated UGT2B7 as the major member of the UGT2B family in the rat liver[48]. Our study showed that an anti-UGT2B7 antibody markedly inhibited glucuronidation of AZT in rat hepatic microsomes. The estimated contribution of UGT2B7 to total AZT glucuronidation was approximately 52%, thus indicating that, as in humans, UGT2B7 in rats is responsible for AZT glucuronidation. Subsequently, the hepatic UGT2B7 activity in the hepatic microsomes of ALF rats was measured on the basis of the formation of GAZT. The measured UGT2B7 activity in ALF rats was only approximately 70% of that in the control rats, in agreement with the decrease in protein expression of hepatic UGT2B7. These results were consistent with the findings in patients with liver disease[49, 50]. The intestinal metabolism of AZT was also taken into consideration because UGT2B7 is also expressed in the intestine[51], but the formation of GAZT in intestinal microsomes was not detected. These results revealed that the impaired hepatic UGT2B7 expression and activity induced by ALF contributed to the increased exposure of AZT after oral and intravenous administration.

The mechanism involved in the suppression of UGT2B7 expression during ALF is not fully understood. Several reports have shown that proinflammatory and inflammatory cytokines might down-regulate CYP450s, transporters and

UDP-glucuronosyltransferases[52-54]. A recent study has also found that increases in a group of inflammatory cytokines (interleukin-4, interleukin-5, and interleukin-13) are associated with a significant decline in the UGT1A1, UGT1A9, and UGT2B5 mRNAs in the Schistosoma-infected mouse model[55], thus indicating that the elevated inflammatory cytokines induced by ALF may explain the suppressed UGT2B7 expression. This possibility was partly supported by the current finding that TNF-α levels were significantly increased in ALF rats. In addition, ALF is often associated with oxidative stress, on the basis of the observation that decreased levels of GSH-Px and CAT and increased levels of MDA were induced in the livers of ALF rats. Moreover, oxidative stress has been reported to inhibit the catalytic functions of UGT1A6 and UGT1A7 in rat astrocytes[56], thus suggesting a role of oxidative stress in the suppression of hepatic UGT2B7 in ALF rats; further investigation is needed.

Interestingly, ALF rats not only had a greater C_{max} (7.76±0.88 μg/mL in ALF rats *vs* 5.72±0.70 μg/mL in control rats, $P<0.01$) but also had a shorter T_{max} (0.54±0.10 h in ALF rats *vs* 0.71±0.10 h in control rats, $P<0.05$) after oral administration of AZT, thus suggesting enhancement of AZT absorption under the ALF condition. Data from the *in situ* single-pass perfusion showed that ALF significantly increased the oral absorption of AZT across the intestinal wall. The histopathological assessment demonstrated that the intestinal physiological structure and integrity of the ALF rats remained intact, thus excluding the possibility that damaged intestinal integrity might contribute to the increased oral absorption of AZT across the intestine.

P-gp and BCRP are responsible for the efflux of AZT from intestinal cells[57]. P-gp has been reported to limit the absorption of multiple drugs, including AZT, through rat intestinal segments[58-60]. An *in vitro* study using Caco-2 and MDCK-MDR1 cells has also demonstrated that AZT is a substrate of P-gp[22]. In addition, $CD4^+$ and $CD8^+$ T cells from patients with HIV-1 infections exhibit greater accumulation of AZT, accompanied by suppressed expression of P-gp[61]. AZT is also a substrate of BCRP, as evidenced by the decreased AZT uptake reported in BCRP-overexpressing MDCK II cells[21]. Together, these results indicate that the attenuated function and expression of P-gp and BCRP might contribute to the increased oral absorption of AZT in ALF rats. However, data from the Western blots clearly revealed that ALF decreased the expression of intestinal P-gp, not BCRP, a result consistent with the impaired intestinal P-gp function (increased oral absorption of rhodamine 123). Together, these results indicated that the attenuated function and expression of P-gp, at least in part, contributed to the enhanced oral absorption of AZT in ALF rats.

Our previous studies have verified that hyperammonemia increases the function and expression of P-gp at the blood-brain barrier by activating the NF-κB pathway[35] and that ALF impairs the function and expression of BCRP at the blood-brain barrier partly by activating the ammonia-ROS-ERK1/2 pathway[23]. These results indicate tissue-specific alterations in the expression and function of P-gp and BCRP in ALF rats. However, the underlying mechanisms remain obscure and require further investigation.

In addition to hepatic UGT2B7, intestinal P-gp and BCRP were found to be involved in the alteration of the pharmacokinetic behavior of AZT in ALF rats. Several other factors may also result in a higher oral exposure of AZT under ALF. Previous studies have documented that organic anion transporters (OATs) including OAT1, OAT2 and OAT3 participate in the transport of AZT in the liver and kidney[62]. The rat OAT1 protein is primarily expressed in the basolateral membrane of renal proximal tubule cells and is responsible for transferring AZT from the blood into proximal tubule cells. Rat OAT2, which is abundantly expressed in the liver, regulates AZT uptake into hepatocytes[63]. The rat OAT3 protein localization was similar to that of OAT1 and facilitated uptake of AZT from the blood into proximal tubule cells. However, in a comparative study on murine OAT1 and OAT3, most antiviral agents including AZT have been found to have a higher affinity for OAT1[64], thus suggesting that OAT3 is of limited importance in the renal secretion of AZT. Our results showed that ALF did not alter urinary excretion of AZT or its metabolite, GAZT, thus suggesting that the functions of OAT1 and OAT3 in renal proximal tubule cells may not be changed by ALF. Decreased hepatic OAT2 activity and expression may also contribute to the higher oral exposure of AZT in ALF rats observed in this study, as evidenced by the decrease in liver OAT2 expression found in chronic hepatitis C patients[65].

In conclusion, the oral plasma exposure of AZT was significantly increased in TAA-induced ALF rats, possibly as a result of the decreased function and expression of intestinal P-gp and hepatic UGT2B7 under ALF conditions. Because AZT displays mitochondrial toxicities in a wide array of organs and tissues, more attention should be paid to the use of AZT in patients with liver failure.

Acknowledgements

This work was supported by the National Natural Science Foundation of China (No 81373482 and 81573490), the Natural Science Foundation of Jiangsu Province (No BK20161457) and the "Six Talent Peaks" Project of Jiangsu Province.

Author contribution

Li LIU and Fan WANG designed the experiments and analyzed the data; Li LIU and Fan WANG wrote the paper; Xiao-dong LIU revised the paper; Fan WANG, Ming-xing MIAO, Bin-bin SUN, Zhong-jian WANG, Xian-ge TANG, Yang CHEN, and Kai-jing ZHAO performed the research.

References

1 Dietrich CG, Gotze O, Geier A. Molecular changes in hepatic metabolism and transport in cirrhosis and their functional importance. World J Gastroenterol 2016; 22: 72–88.

2 George J, Liddle C, Murray M, Byth K, Farrell GC. Pretranslational regulation of cytochrome-p450 genes is responsible for disease-specific changes of individual p450 enzymes among patients with cirrhosis. Biochem Pharmacol 1995; 49: 873–81.

3 George J, Murray M, Byth K, Farrell GC. Differential alterations of cytochrome P450 proteins in livers from patients with severe chronic liver disease. Hepatology 1995; 21: 120–8.
4 Yalcin EB, More V, Neira KL, Lu ZQ, Cherrington NJ, Slitt AL, *et al*. Downregulation of sulfotransferase expression and activity in diseased human livers. Drug Metab Dispos 2013; 41: 1642–50.
5 More VR, Cheng QQ, Donepudi AC, Buckley DB, Lu ZJ, Cherrington NJ, *et al*. Alcohol cirrhosis alters nuclear receptor and drug transporter expression in human liver. Drug Metab Dispos 2013; 41: 1148–55.
6 Wyles DL, Gerber JG. Antiretroviral drug pharmacokinetics in hepatitis with hepatic dysfunction. Clin Infect Dis 2005; 40: 174–81.
7 Broder S. The development of antiretroviral therapy and its impact on the HIV-1/AIDS pandemic. Antivir Res 2010; 85: 1–18.
8 Gunthard HF, Aberg JA, Eron JJ, Hoy JF, Telenti A, Benson CA, *et al*. Antiretroviral Treatment of Adult HIV Infection 2014 Recommendations of the International Antiviral Society-USA Panel. JAMA 2014; 312: 410–25.
9 Clumeck N, Pozniak A, Raffi F, Committee EE. European AIDS Clinical Society (EACS) guidelines for the clinical management and treatment of HIV-infected adults. Hiv Med 2008; 9: 65–71.
10 Mulenga V, Musiime V, Kekitiinwa A, Cook AD, Abongomera G, Kenny J, *et al*. Abacavir, zidovudine, or stavudine as paediatric tablets for African HIV-infected children (CHAPAS-3): an open-label, parallel-group, randomised controlled trial. Lancet Infect Dis 2016; 16: 169–79.
11 Mu L, Zhou R, Tang F, Liu X, Li S, Xie F, *et al.* Intracellular pharmacokinetic study of zidovudine and its phosphorylated metabolites. Acta Pharm Sin B 2016; 6: 158–62.
12 Serra CHDR, Koono EEM, Kano EK, Schramm SG, Armando YP, Porta V. Bioequivalence and pharmacokinetics of two zidovudine formulations in healthy Brazilian volunteers: An open-label, randomized, single-dose, two-way crossover study. Clin Ther 2008; 30: 902–8.
13 Veal GJ, Back DJ. Metabolism of zidovudine. Gen Pharmacol 1995; 26: 1469–75.
14 Barbier O, Turgeon D, Girard C, Green MD, Tephly TR, Hum DW, *et al*. 3'-azido-3'-deoxythimidine (AZT) is glucuronidated by human UDP-glucuronosyltransferase 2B7 (UGT2B7). Drug Metab Dispos 2000; 28: 497–502.
15 Court MH. Enzyme-selective probe substrates for *in vitro* studies of human UDP-glucuronosyltransferases. Methods Enzymol 2005; 400: 104–16.
16 Child S, Montaner J, Tsoukas C, Fanning M, Le T, Wall RA, *et al*. Canadian multicenter azidothymidine trial: AZT pharmacokinetics. J Acquir Immune Defic Syndr 1991; 4: 865–70.
17 Taburet AM, Naveau S, Zorza G, Colin JN, Delfraissy JF, Chaput JC, *et al*. Pharmacokinetics of zidovudine in patients with liver cirrhosis. Clin Pharmacol Ther 1990; 47: 731–9.
18 Moore KH, Raasch RH, Brouwer KL, Opheim K, Cheeseman SH, Eyster E, *et al*. Pharmacokinetics and bioavailability of zidovudine and its glucuronidated metabolite in patients with human immunodeficiency virus infection and hepatic disease (AIDS Clinical Trials Group protocol 062). Antimicrob Agents Chemother 1995; 39: 2732–7.
19 Furlan V, Demirdjian S, Bourdon O, Magdalou J, Taburet AM. Glucuronidation of drugs by hepatic microsomes derived from healthy and cirrhotic human livers. J Pharmacol Exp Ther 1999; 289: 1169–75.
20 Dalpiaz A, Fogagnolo M, Ferraro L, Capuzzo A, Pavan B, Rassu G, *et al*. Nasal chitosan microparticles target a zidovudine prodrug to brain HIV sanctuaries. Antiviral Res 2015; 123: 146–57.
21 Pan G, Giri N, Elmquist WF. Abcg2/Bcrp1 mediates the polarized transport of antiretroviral nucleosides abacavir and zidovudine. Drug Metab Dispos 2007; 35: 1165–73.
22 De Souza J, Benet LZ, Huang Y, Storpirtis S. Comparison of bidirectional lamivudine and zidovudine transport using MDCK, MDCK-MDR1, and caco-2 cell monolayers. J Pharm Sci 2009; 98: 4413–9.
23 Li Y, Zhang J, Xu P, Sun BB, Zhong ZY, Liu C, *et al*. Acute liver failure impairs function and expression of breast cancer-resistant protein (BCRP) at rat blood-brain barrier partly via ammonia-ROS-ERK1/2 activation. J Neurochem 2016; 138: 282–94.
24 Jin S, Wang XT, Liu L, Yao D, Liu C, Zhang M, *et al*. P-glycoprotein and multidrug resistance-associated protein 2 are oppositely altered in brain of rats with thioacetamide-induced acute liver failure. Liver Int 2013; 33: 274–82.
25 Sathyasaikumar KV, Swapna I, Reddy PVB, Murthy CRK, Roy KR, Gupta AD, *et al*. Co-administration of C-phycocyanin ameliorates thioacetamide-induced hepatic encephalopathy in Wistar rats. J Neurol Sci 2007; 252: 67–75.
26 Farjam M, Dehdab P, Abbassnia F, Mehrabani D, Tanideh N, Pakbaz S, *et al*. Thioacetamide-induced acute hepatic encephalopathy in rat: behavioral, biochemical and histological changes. Iran Red Crescent Med J 2012; 14: 164–70.
27 Sun H, Zhang T, Wu Z, Wu B. Warfarin is an effective modifier of multiple UDP-glucuronosyltransferase enzymes: evaluation of its potential to alter the pharmacokinetics of zidovudine. J Pharm Sci 2015; 104: 244–56.
28 Quevedo MA, Briñón MC. *In vitro* and *in vivo* pharmacokinetic characterization of two novel prodrugs of zidovudine. Antiviral Res 2009; 83: 103–11.
29 Wannachaiyasit S, Chanvorachote P, Nimmannit U. A novel anti-HIV dextrin-zidovudine conjugate improving the pharmacokinetics of zidovudine in rats. AAPS Pharm Sci Tech 2008; 9: 840–50.
30 Liu H, Liu L, Li J, Mei D, Duan R, Hu N, *et al*. Combined contributions of impaired hepatic cyp2c11 and intestinal bcrp activities and expressions to increased exposure of oral glibenclamide in streptozotocin-induced diabetic rats. Drug Metab Dispos 2012; 40: 1104–12.
31 Mano Y, Usui T, Kamimura H. Comparison of inhibition potentials of drugs against zidovudine glucuronidation in rat hepatocytes and liver microsomes. Drug Metab Dispos 2007; 35: 602–6.
32 Court MH, Krishnaswamy S, Hao Q, Duan SX, Patten CJ, Von Moltke LL, *et al*. Evaluation of 3'-azido-3'-deoxythymidine, morphine, and codeine as probe substrates for UDP-glucuronosyltransferase 2B7 (UGT2B7) in human liver microsomes: Specificity and influence of the UGT2B7*2 polymorphism. Drug Metab Dispos 2003; 31: 1125–33.
33 Zhang J, Zhang M, Sun B, Li Y, Xu P, Liu C, *et al*. Hyperammonemia enhances the function and expression of P-glycoprotein and Mrp2 at the blood-brain barrier through NF-κB. J Neurochem 2014; 131: 791–802.
34 Liu YC, Liu HY, Yang HW, Wen T, Shang Y, Liu XD, *et al*. Impaired expression and function of breast cancer resistance protein (Bcrp) in brain cortex of streptozocin-induced diabetic rats. Biochem Pharmacol 2007; 74: 1766–72.
35 Zhong ZY, Sun BB, Shu N, Xie QS, Tang XG, Ling ZL, *et al*. Ciprofloxacin blocked enterohepatic circulation of diclofenac and alleviated NSAID-induced enteropathy in rats partly by inhibiting intestinal β-glucuronidase activity. Acta Pharmacol Sin 2016; 37: 1002–12.
36 Sutton SC, Rinaldi MT, Vukovinsky KE. Comparison of the gravimetric, phenol red, and ^{14}C-PEG-3350 methods to determine water absorption in the rat single-pass intestinal perfusion model. AAPS PharmSci 2001; 3: E25.
37 Ramalhosa F, Soares-Cunha C, Seixal RM, Sousa N, Carvalho AF. The

impact of prenatal exposure to dexamethasone on gastrointestinal function in rats. PLoS One 2016; 11: e0161750.
38 Divi RL, Doerge DR, Twaddle NC, Shockley ME, St Claire MC, St Claire MC, *et al*. Metabolism and pharmacokinetics of the combination Zidovudine plus Lamivudine in the adult Erythrocebus patas monkey determined by liquid chromatography-tandem mass spectrometric analysis. Toxicol Appl Pharmacol. 2008; 226: 206–11.
39 Liu H, Sun H, Lu D, Zhang Y, Zhang X, Ma Z, *et al*. Identification of glucuronidation and biliary excretion as the main mechanisms for gossypol clearance: *in vivo* and *in vitro* evidence. Xenobiotica 2014; 44: 696–707.
40 Marier JF, Manthos H, Kebir S, Ferron S, DiMarco M, Morelli G, *et al*. Comparative bioavailability study of zidovudine administered as two different tablet formulations in healthy adult subjects. Int J Clin Pharm Th 2006; 44: 240–6.
41 Liu X, Yang Z, Yang J, Yang H. Increased P-glycoprotein expression and decreased phenobarbital distribution in the brain of pentylenetetrazole-kindled rats. Neuropharmacology 2007; 53: 657–63.
42 Mays DC, Dixon KF, Balboa A, Pawluk LJ, Bauer MR, Nawoot S, *et al*. A nonprimate animal model applicable to zidovudine pharmacokinetics in humans: inhibition of glucuronidation and renal excretion of zidovudine by probenecid in rats. J Pharmacol Exp Ther 1991; 259: 1261–70.
43 de Miranda P, Burnette TC, Good SS. Tissue distribution and metabolic disposition of zidovudine in rats. Drug Metab Dispos 1990; 18: 315–20.
44 Faleiros BE, Miranda AS, Campos AC, Gomides LF, Kangussu LM, Guatimosim C, *et al*. Up-regulation of brain cytokines and chemokines mediates neurotoxicity in early acute liver failure by a mechanism independent of microglial activation. Brain Res 2014; 1578: 49–59.
45 Wyles DL, Gerber JG. Antiretroviral drug pharmacokinetics in hepatitis with hepatic dysfunction. Clin Infect Dis 2005; 40: 174–81.
46 Chatton JY, Munafo A, Chave JP, Steinhäuslin F, Roch-Ramel F, Glauser MP, *et al*. Trimethoprim, alone or in combination with sulphamethoxazole, decreases the renal excretion of zidovudine and its glucuronide. Br J Clin Pharmacol 1992; 34: 551–4.
47 Wang LH, Chittick GE, McDowell JA. Single-dose pharmacokinetics and safety of abacavir (1592U89), zidovudine, and lamivudine administered alone and in combination in adults with human immunodeficiency virus infection. Antimicrob Agents Chemother 1999; 43: 1708–15.
48 Anderson GD, Peterson TC, Vonder Haar C, Farin FM, Bammler TK, MacDonald JW, *et al*. Effect of traumatic brain injury, erythropoietin, and anakinra on hepatic metabolizing enzymes and transporters in an experimental rat model. AAPS J 2015; 17: 1255–67.
49 Lu L, Zhou J, Shi J, Peng XJ, Qi XX, Wang Y, *et al*. Drug-metabolizing activity, protein and gene expression of UDP-glucuronosyltransferases are significantly altered in hepatocellular carcinoma patients. PLoS One 2015; 10: e0127524.
50 Congiu M, Mashford ML, Slavin JL, Desmond PV. UDP glucuronosyltransferase mRNA levels in human liver disease. Drug Metab Dispos 2002; 30: 129–34.
51 Zhu L, Ge G, Liu Y, Guo Z, Peng C, Zhang F, *et al*. Characterization of UDP-glucuronosyltransferases involved in glucuronidation of diethylstilbestrol in human liver and intestine. Chem Res Toxicol 2012; 25: 2663–9.
52 Morgan ET, Goralski KB, Piquette-Miller M, Renton KW, Robertson GR, Chaluvadi MR, *et al*. Regulation of drug-metabolizing enzymes and transporters in infection, inflammation, and cancer. Drug Metab Dispos 2008; 36: 205–16.
53 Morgan ET. Impact of infectious and inflammatory disease on cytochrome P450-mediated drug metabolism and pharmacokinetics. Clin Pharmacol Ther 2009; 85: 434–8.
54 Richardson TA, Sherman M, Kalman D, Morgan ET. Expression of UDP-glucuronosyltransferase isoform mRNAs during inflammation and infection in mouse liver and kidney. Drug Metab Dispos 2006; 34: 351–3.
55 Mimche SM, Nyagode BA, Merrell MD, Lee CM, Prasanphanich NS, Cummings RD, *et al*. Hepatic cytochrome P450s, phase II enzymes and nuclear receptors are downregulated in a Th2 environment during *Schistosoma mansoni* infection. Drug Metab Dispos 2014; 42: 134–40.
56 Gradinaru D, Minn AL, Artur Y, Minn A, Heydel JM. Effect of oxidative stress on UDP-glucuronosyltransferases in rat astrocytes. Toxicol Lett 2012; 213: 316–24.
57 Neumanova Z, Cerveny L, Ceckova M, Staud F. Role of ABCB1, ABCG2, ABCC2 and ABCC5 transporters in placental passage of zidovudine. Biopharm Drug Dispos 2016; 37: 28–38.
58 Jia Y, Liu Z, Wang C, Meng Q, Huo X, Liu Q, *et al*. P-gp, MRP2 and OAT1/OAT3 mediate the drug-drug interaction between resveratrol and methotrexate. Toxicol Appl Pharmacol 2016; 306: 27–35.
59 Huo X, Liu Q, Wang C, Meng Q, Sun H, Peng J, *et al*. Enhancement effect of P-gp inhibitors on the intestinal absorption and antiproliferative activity of bestatin. Eur J Pharm Sci 2013; 50: 420–8.
60 Quevedo MA, Nieto LE, Brinon MC. P-glycoprotein limits the absorption of the anti-HIV drug zidovudine through rat intestinal segments. Eur J Pharm Sci 2011; 43: 151–9.
61 Andreana A, Aggarwal S, Gollapudi S, Wien D, Tsuruo T, Gupta S. Abnormal expression of a 170-kilodalton P-glycoprotein encoded by MDR1 gene, a metabolically active efflux pump, in $CD4^+$ and $CD8^+$ T cells from patients with human immunodeficiency virus type 1 infection. AIDS Res Hum Retroviruses 1996; 12: 1457–62.
62 Burckhardt G. Drug transport by organic anion transporters (OATs). Pharmacol Ther 2012; 136: 106–30.
63 Morita N, Kusuhara H, Sekine T, Endou H, Sugiyama Y. Functional characterization of rat organic anion transporter 2 in LLC-PK1 cells. J Pharmacol Exp Ther 2001; 298: 1179–84.
64 Truong DM, Kaler G, Khandelwal A, Swaan PW, Nigam SK. Multi-level analysis of organic anion transporters 1, 3, and 6 reveals major differences instructural determinants of antiviral discrimination. J Biol Chem 2008; 283: 8654–63.
65 Yasui Y, Kudo A, Kurosaki M, Matsuda S, Muraoka M, Tamaki N, *et al*. Reduced organic anion transporter expression is a risk factor for hepatocellular carcinoma in chronic hepatitis C patients: a propensity score matching study. Oncology 2014; 86: 53–62.